NANOFLUID ENHANCED OIL RECOVERY – MOBILITY RATIO, SURFACE CHEMISTRY, OR BOTH?

A. Khezrnejad, L.A. James, T.E. Johansen
Memorial University of Newfoundland

This paper was prepared for presentation at the International Symposium of the Society of Core Analysts held in St. John's Newfoundland and Labrador, Canada, 16-21 August, 2015

ABSTRACT

The goal of enhanced oil recovery (EOR) is to manipulate the fluid-fluid properties and fluid-rock properties between the injected fluid and the residual oil phase to improve recovery efficiency. Water enhanced with nanoparticles (nanofluids) has recently gained research interest for enhanced oil recovery because of the possible physical and chemical properties imparted by the nanoparticles. The application of nanofluids in enhanced oil recovery is strongly dependent on the resulting nanofluid properties. The research question asked is whether oil recovery using nanoparticle enhanced water is due to a more favorable mobility ratio (increased water phase viscosity) or is it due to the effect of the enhanced surface chemistry? In this study, we examine the role of increased viscosity of the water phase on oil recovery using nanoparticle enhanced water and polymer enhanced water with similar viscosity. First, the nanoparticle enhanced water is characterized. A statistical design of experiments technique, Response Surface Methodology, is used to investigate the effect of the type of nanoparticles (silicon oxide and aluminum oxide nanoparticles), concentration of the nanoparticles, pressure, and temperature on viscosity. The effect of interactions between the factors on viscosity is also studied. Second, the viscosity measurement results are used to plan micromodel and coreflooding laboratory scale enhanced oil recovery experiments at low pressure and temperature conditions. The results can be used to help elucidate the role of increasing viscosity versus surface chemistry on oil recovery.

INTRODUCTION

The two main forces controlling fluid flow in porous media are viscous and capillary forces. Literature suggests that recovery efficiency can be improved for waterflooding by increasing the viscosity of injected fluid (improving the macroscopic sweep efficiency) or through improving the microscopic efficiency via wettability alteration or interfacial tension reduction [1, 2, 3].

Polymers are commonly used to increase viscosity of the injected phase [4, 5, 6, 7]. However, challenges such as the stability of polymers in harsh reservoir conditions, cost, and required facilities hinder the wider use of polymer flooding [8, 9]. Adding nanoparticles to water increases the viscosity; hence, improves the mobility ratio [10, 11]. Nanofluids have been shown to be very effective in terms of wettability alteration and interfacial tension reduction [12, 13, 14]. Moreover, Zhang et al. [15] along with other

researchers demonstrated that specially designed nanoparticles are significantly more stable than polymers or surfactants in harsh reservoir conditions [16, 17]. All these features make nanofluids a very promising EOR technique for improving both microscopic and macroscopic sweep efficiency.

In this study, nanoparticle enhanced water flooding is compared to polymer enhanced water flooding to examine the role of mobility ratio, surface chemistry or both on oil recovery efficiency. Two different types of nanoparticles were added to deionized (DI). The results of the nanoparticle enhanced water flooding experiments are compared to polymer flooding using a polymer solution with the same viscosity as the nanofluid. Moreover, response surface methodology, a statistical design of experiment technique, was used to investigate the effect of nanoparticle concentration, pressure, and temperature on the viscosity of DI water. The effect of interactions between the factors on the viscosity was also studied. Interfacial tension between the nanofluid and oil, and the polymer solution and oil were also measured to better understand the possible mechanisms of oil recovery.

MICROMODEL EXPERIMENTS

Etched micromodels were used to examine the effectiveness of injecting nanoparticle enhanced water and polymer water solutions on oil recovery. The properties of the dispersed nanoparticles (manufactured by US Research Nanomaterials, Inc.) are tabulated in Table 1. It should be noted that the silica (SiO_2) nanoparticles used in the experiments were amorphous, and the alumina (Al_2O_3) nanoparticles were gamma type. In order to completely disperse the nanoparticles in the DI water, an ultrasonic device was used. The sonication process was performed on the nanofluid for 30 minutes. Homogeneity and stability of the prepared solution were confirmed by placing the nanofluid solution in a closed transparent bottle away from degrading factors such as light and heat for two weeks. Visual inspection showed neither precipitation nor other visible alterations indicating a stable nanoparticle suspension. The polymer used in these set of experiments was Flopaam 3430S (manufactured by SNF Floerger). The hydrocarbon fluid used in the experiments was stock tank crude oil from offshore Newfoundland with approximately 32-35 ºAPI.

Table 1: Properties of nanoparticles

Type	Description	Average Particle Size (nm)	Purity (%)	pH value
Al_2O_3	Gamma	10	99.9	2-5
SiO_2	Amorphous	5-35	99.9	8-11

A micromodel fabricated from polymethyl methacrylate (PMMA) was used as the porous medium. Figure 1 shows a photo of the micromodel saturated with oil. Table 2 shows the properties of the micromodel. Different scenarios of waterflooding were performed on the glass micromodel using: DI water, polymer solution, silica nanofluid (5 wt%), and alumina nanofluid (5 wt%). Figure 2 shows a schematic of the micromodel visualization setup. The different injection scenarios are defined in Table 3.

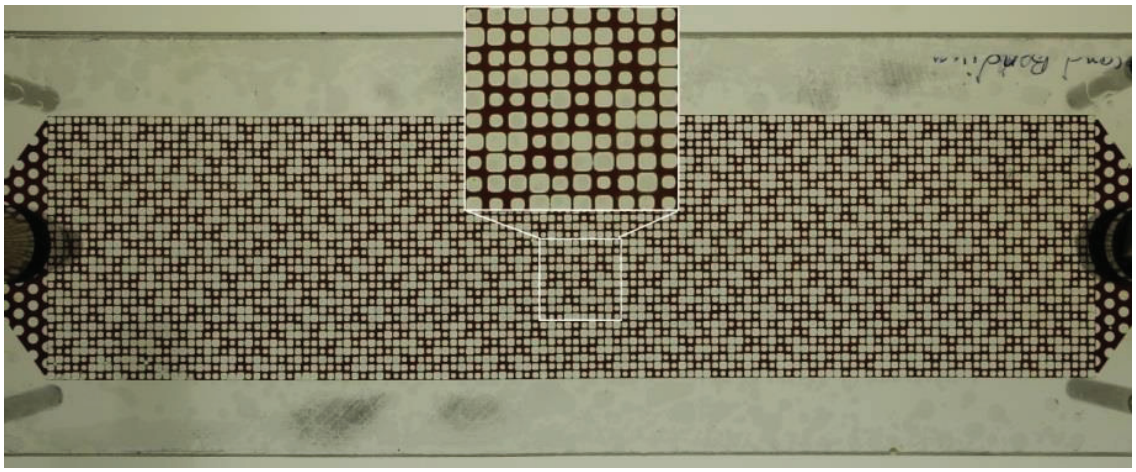

Figure 1: PMMA Micromodel

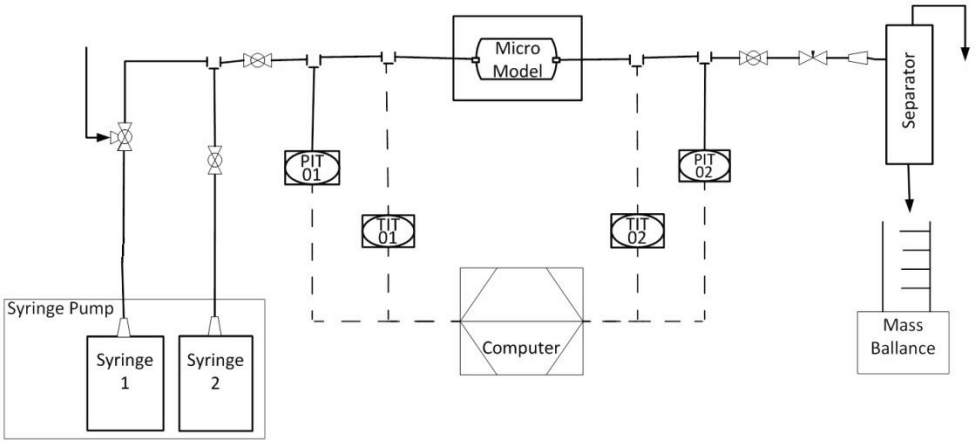

Figure 2: Schematic diagram of micromodel visualization setup

The following procedure was used to conduct the nanofluid/polymer solution/DI waterflooding experiments in the low pressure (ambient conditions) micromodel system:

1. The micromodel was cleaned by flushing with hexane (2 pore volumes).
2. The micromodel was completely dried using compressed air.
3. The injection fluids were loaded in the syringe pumps.
4. DI water was injected up to the inlet through the temporary line.
5. The micromodel inlet valve was closed.
6. The micromodel and downstream tubing were vacuumed to remove any air and reduce the probability of trapping air during the primary imbibition.
7. The outlet valve was closed.
8. By opening the inlet, the system was drained by DI water.
9. The outlet valve was opened.
10. Oil was loaded into a temporary line.
11. Oil was injected into the micromodel to the outlet.
12. Slugs of desired fluid were injected in the micromodel.

Table 2: Micromodel dimensions and characteristics

Description	Dimension
Length (cm)	25.6
Width (cm)	6.4
Average depth (μm)	160
Porosity	0.43
Pore Volume (cm^3)	1.15
Permeability (Darcy)	2.9

Table 3: Micromodel Experimental Conditions

Test #	Injected Fluid	Viscosity (cP)	Injection flow rate (ml/min)
1	DI water	1.00	0.010
2	Polymer (10 ppm)	1.75	0.010
3	Polymer (10 ppm)	1.75	0.005
4	Polymer (10 ppm)	1.75	0.010
5	Polymer (20 ppm)	2.30	0.010
6	Polymer (20 ppm)	2.30	0.005
7	SiO_2 nanofluid (5 wt%)	1.06	0.010
8	Al_2O_3 nanofluid (5 wt%)	1.75	0.010

Oil saturation in the micromodel experiments can be measured at any time by image analysis. Standard image analysis using Matlab software® was used to determine the oil recovery. The difference between the initial state of the black pixels and the final state was interpreted as oil recovery.

Figure 3 shows the oil recovery at different pore volumes injected. The recovery values used for the polymer 10 ppm case are the average value of test # 2 and 4. The standard deviation was measured to be 1.89% recovery according to recovery values measured for these two tests. The standard deviation is also shown in Figure 3. As shown in the figure, the recovery values for alumina, silica and DI water are outside of this standard deviation giving us confidence in the experimental results. Comparing the recovery of alumina nanofluid and polymer solution (10 ppm) both with μ = 1.75 cP at experimental conditions, we can see that the oil recovery for the alumina nanofluid is higher. Moreover, we can see that silica nanofluid with μ=1.06 cP but the lowest interfacial tension (will be discussed more) has the highest oil recovery. This higher oil recovery might result from improvement of microscopic sweep efficiency. Nanoparticles have the ability to decrease the interfacial tension between oil and water and improve microscopic efficiency, which will be discussed in detail in IFT measurements section later.

Figure 4 shows the ultimate oil recovery, oil recovery at breakthrough, and breakthrough time for different injection scenarios. As shown in the figure, oil recoveries obtained for the alumina and silica nanofluids are 8 and 11% higher than the oil recovery by DI water injection respectively, showing a significant improvement of oil recovery. Moreover, the recoveries from injecting alumina and silica nanofluids were 5 and 8% higher respectively than the recovery from injecting 10 ppm polymer. The oil recovery from injecting 10 ppm polymer compared to DI water injection was approximately 3% higher, which illustrates the effect of the increased viscosity of the injected fluid on oil recovery. As shown in Figure 4, injected fluids with the same viscosities have approximately the same breakthrough time.

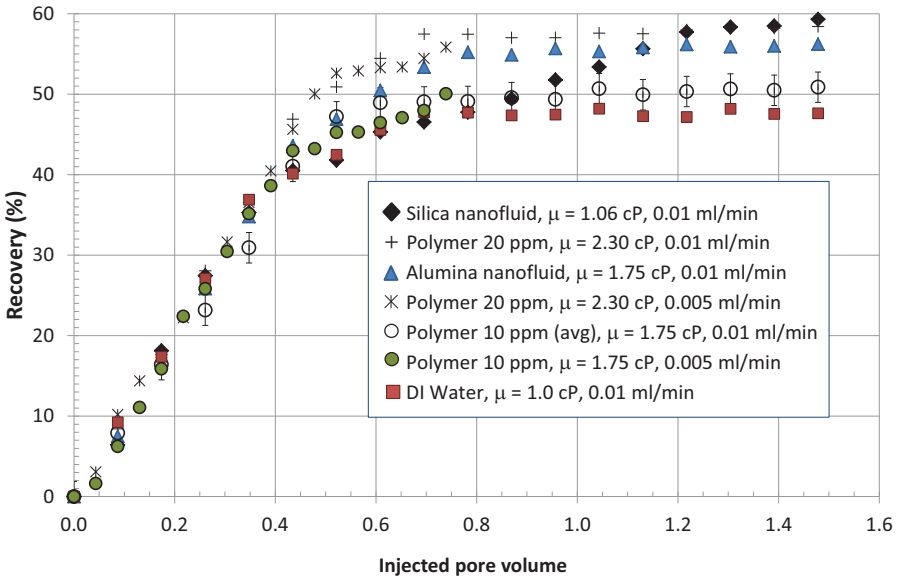

Figure 3: Oil Recovery vs. injected pore volume

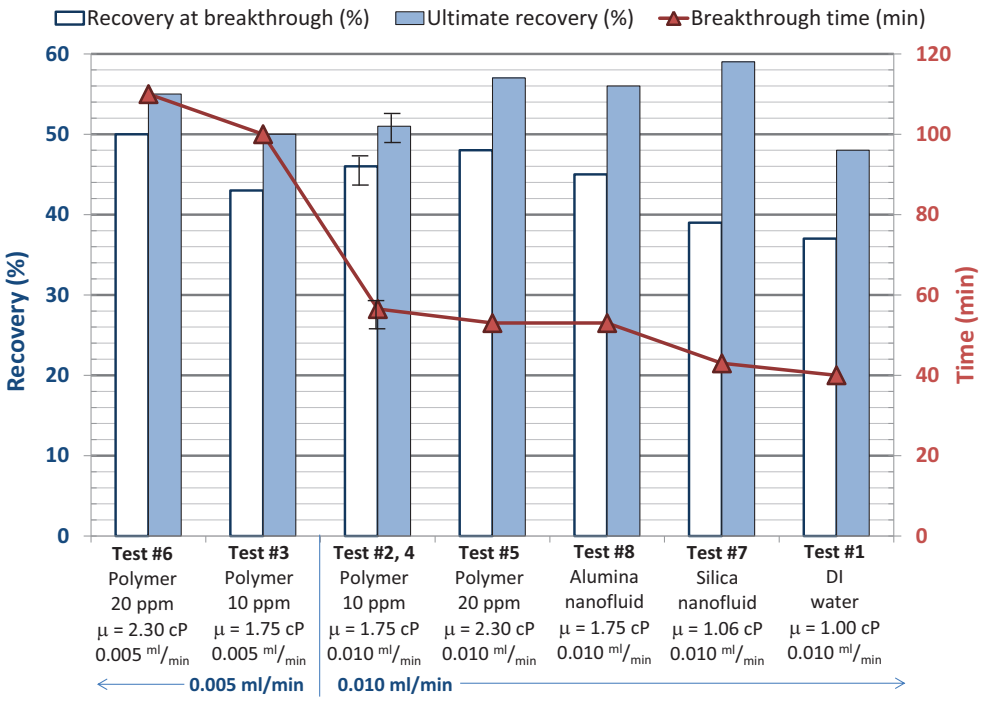

Figure 4: Ultimate recovery, recovery at breakthrough, and breakthrough time for the experiments

One replicate test was performed for the polymer (10 ppm) solution to better estimate the error in the experiments. The difference in recovery of tests two and four with a polymer concentration of 10 ppm at 0.010 ml/min was approximately 2%. This difference in recoveries might be due to experimental errors or image analysis errors. An additional experiment at half flow rate was also performed to see the effect of flow rate on

breakthrough time and ultimate recovery. Decreasing the injection flow rate causes a more stable front movement, which increases the breakthrough time significantly. However, ultimate recovery did not change by decreasing the flow rate.

Overall, nanofluid injection has higher recovery compared to polymer waterflooding. The fact that nanoparticles are surface active at the oil-water interface might be the reason for this improvement. Therefore, we measured the interfacial tension between the nanofluid and oil as well as the interfacial tension between the polymer solution and oil to better understand the role of nanoparticles in possibly reducing the interfacial tension between the immiscible phases. This is discussed in more detail subsequently. Mobility control might be another reason for enhanced oil recovery of nanofluid or polymer injection over simple water flooding. In the next section the viscosity measurements for nanofluid, polymer solution and DI water are discussed.

NANOFLUID VISCOSITY MEASUREMENTS

As discussed in the introduction, nanoparticles are capable of increasing the viscosity of water. However, most of these viscosity measurements were conducted under fixed pressure and temperature. In order to understand the behavior of viscosity with respect to different factors and their interactions, we need to change all the factors at the same time. Response surface methodology (optimal design) was employed to investigate the effect of each factor: concentration of nanoparticles, pressure, temperature, nanoparticle type, and their interaction on the response (viscosity).

In this study, Design Expert Software® was used for the design of experiments. Table 4 shows the 24 viscosity measurements based on optimal design. Concentration, pressure, and temperature are quantitative factors varying from 0 to 5 wt%, 20 to 8000 psia, and 20 to 80°C respectively.

The VISCOlab PVT viscometer (manufactured by Cambridge Viscosity) was used for measuring the viscosity. A billet for the range of 0.25 to 5 cP was used for the experiments. After loading the pump, the system was set to the desired temperature and pressure. Before measuring any data, the system was bled through the relief valves to rid the system of any air. Then, viscosity was measured under stable pressure and temperature conditions. After running each test, the system was flushed with an appropriate solvent to clean all the lines and fittings, and then vacuumed. Bias was avoided by performing the experiments in random order. As shown in the table, * indicates replicate runs. A standard deviation of 0.01cP was calculated based on the replicate values. The viscometer was calibrated using DI water. As shown in Table 4, the viscosity measured for the DI water at ambient condition was 1.07 cP (run #15), which is slightly different than available data for DI water viscosity in literature. This discrepancy might be due to experimental errors.

Table 4: Optimal design of viscosity measurements (* denotes replicate runs)

Run	Concentration (wt%)	Pressure (psia)	Temperature (°C)	Nanoparticle type	Viscosity (cP) ± 0.01
*1	5.00	8000	55.4	Al_2O_3	0.78
*2	5.00	8000	55.4	Al_2O_3	0.80
*3	2.50	4010	50.0	SiO_2	0.66
*4	2.50	4010	50.0	SiO_2	0.66
5	0.00	4110	79.8	DI water	0.36
6	5.00	20	80.0	Al_2O_3	0.53
*7	2.50	4010	50.0	SiO_2	0.66
8	5.00	20	20.0	SiO_2	1.06
9	0.00	4848	22.4	DI water	0.86
10	5.00	4010	24.4	Al_2O_3	1.82
11	5.00	5207	79.8	SiO_2	0.40
*12	2.90	8000	80.0	Al_2O_3	0.40
13	1.85	20	33.8	SiO_2	0.81
14	0.00	8000	22.6	DI water	0.84
15	0.00	20	20.0	DI water	1.07
16	3.80	3611	61.6	Al_2O_3	0.74
17	5.00	8000	21.3	SiO_2	0.92
18	1.00	4010	38.0	Al_2O_3	0.75
*19	2.90	8000	80.0	Al_2O_3	0.43
20	1.43	20	61.7	Al_2O_3	0.51
21	0.00	8000	79.5	DI water	0.34
22	0.00	20	80.4	DI water	0.37
23	0.55	7880	42.5	SiO_2	0.57
24	5.00	4010	27.8	Al_2O_3	1.69

Table 5 shows the analysis of variance (ANOVA) results for the viscosity measurements. The prediction interval provides the upper and lower levels for 95% confidence level. The p-value represents the probability of the occurrence of a given event. When the p-value is less than 0.05 (1-95% confidence) the factor is considered significant. The analysis of variance is model dependent, so it is up to the user to suggest models that describe the data. We systematically tried and compared several different models (linear, quadratic, etc.) with the inclusion and elimination of higher order and interaction terms. The goal was to find the simplest model to best fit the results. The results of the ANOVA table demonstrate that all the individual factors have significant effect on viscosity (p-value < 0.05). Moreover, the interaction between concentration and nanoparticle type and second order terms of pressure and temperature were shown to be important and should be considered in the model.

Figure 5 shows how the viscosity predicted by the model matches the actual experimental data. As shown in the figure, the data points fall very close to the 45° slope line, which confirms that lack of fit is not significant as it was shown in the ANOVA table.

Figure 6 shows the effect of nanoparticles concentration on the viscosity. The black points are indicating the experimental measurements. Figure 6a demonstrates that by

increasing the concentration of alumina (Al_2O_3) nanoparticles in the DI water, the viscosity increases. However, Figure 6b shows that adding silica (SiO_2) nanoparticles to DI water does not change the viscosity significantly. As shown in the figure, viscosity decreases with increasing temperature. The effect of pressure on the viscosity of nanofluid is slightly more significant at lower temperatures. In fact, the viscosity values at high temperature (80°C) are almost the same for different states of pressure, which is showing the insignificance of pressure effect on viscosity at high temperature. The dashed lines indicate the 95% confidence interval bands for the predictive model.

Table 5: Analysis of variance for viscosity experiments

Source	**Sum of Squares**	**Mean Square**	**F Value**	**p-value**
Model	2.320	0.330	359.11	<0.0001
Concentration (C)	0.160	0.160	176.93	<0.0001
Pressure (P)	0.023	0.023	25.09	<0.0001
Temperature (T)	1.840	1.840	1990.49	<0.0001
Nanoparticle type (N)	0.079	0.079	85.15	<0.0001
Concentration x Nanoparticle Type (CN)	0.069	0.069	74.98	<0.0001
$Pressure^2$ (P^2)	0.011	0.011	12.14	0.0021
$Temperature^2$ (T^2)	$4.323x10^{-3}$	$4.323x10^{-3}$	4.68	0.0416
Lack of fit	0.019	$1.096x10^{-3}$	3.26	0.0976

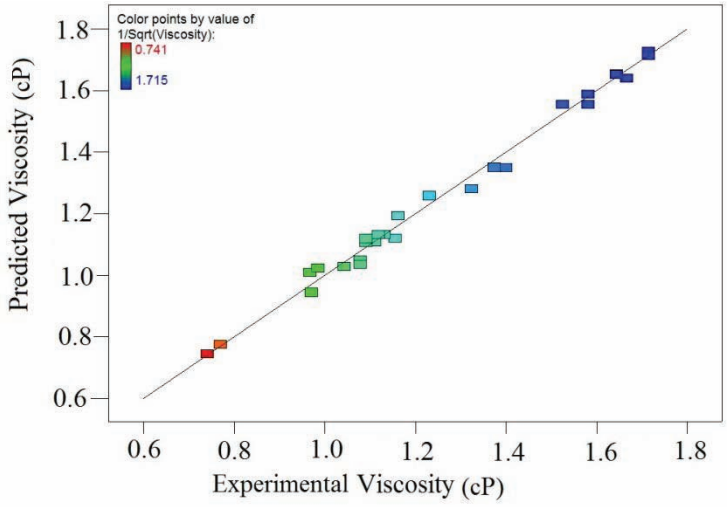

Figure 5: Predicted viscosity vs. experimental viscosity measurements

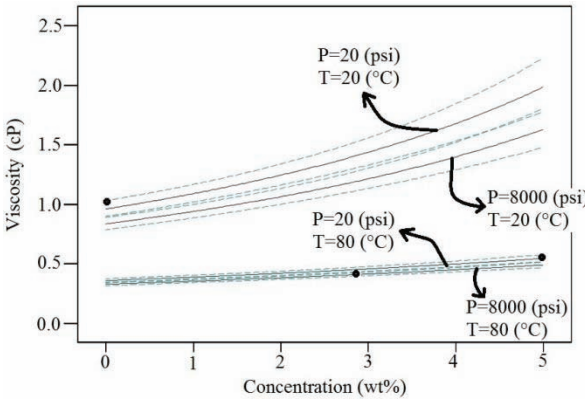

Figure 6a: Effect of nanoparticles concentration on Alumina (Al_2O_3) nanofluid viscosity

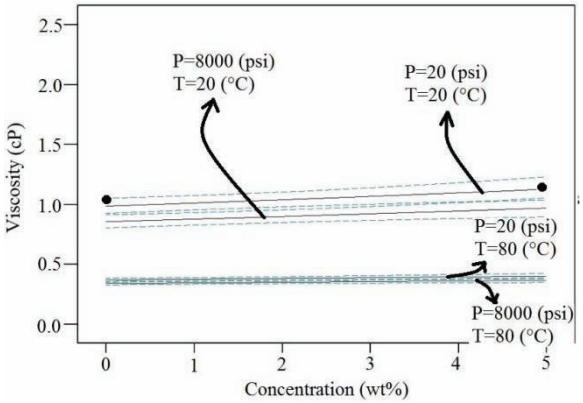

Figure 6b: Effect of nanoparticle concentration on Silica (SiO_2) nanofluid viscosity

Figure 7 shows the effect of interaction between pressure and temperature on the measured viscosity of nanofluid. As shown in the ANOVA table, the effect of second order terms of pressure and temperature are significant. We can see this non-linearity effect in Figure 7. Again, pressure is shown to have little effect. Figure 7b indicates that viscosity behaves more non-linear while using alumina nanoparticles at higher concentration. Moreover, by looking at Figure 7b, we can see that the maximum viscosity was obtained while using alumina nanoparticles at medium pressure, low temperature, and high concentration. For silica nanofluid increasing the concentration of nanoparticles in DI water does not affect the viscosity significantly. However, viscosity increases significantly by increasing the concentration of alumina nanoparticles in DI water. Increasing the concentration of alumina nanoparticles increases the effect of non-linearity behavior of viscosity (Figure 7a and 7b). Overall, the model predicts that the viscosity of DI water can be increased to a maximum value of approximately 2 cP using alumina nanoparticle.

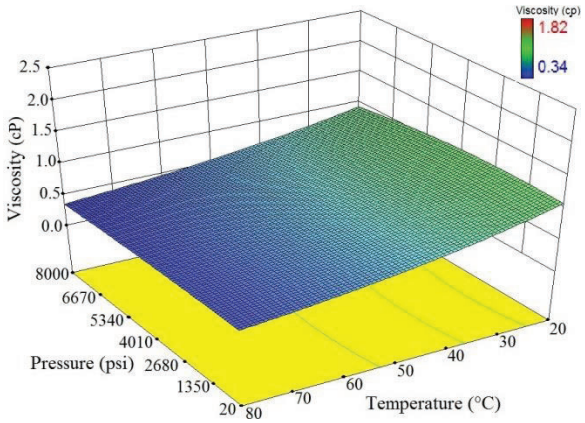

Figure 7a: 3D map of viscosity vs. pressure and temperature (Al_2O_3, 1 wt%)

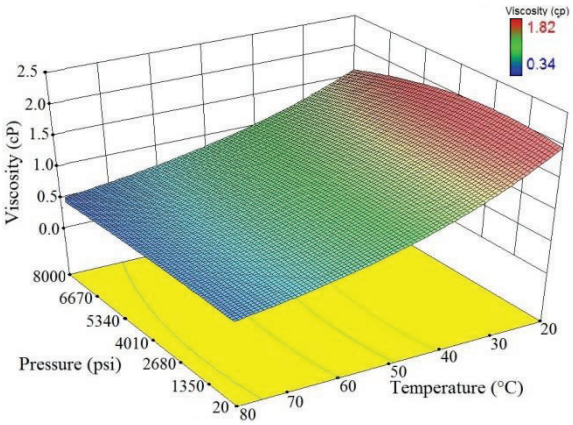

Figure 7b: 3D map of viscosity vs. pressure and temperature (Al_2O_3, 5 wt%)

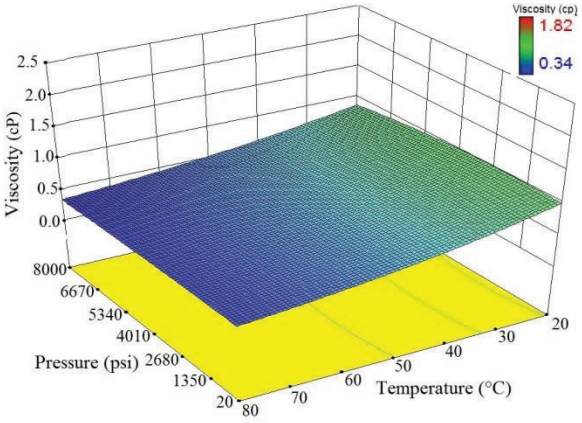

Figure 7c: 3D map of viscosity vs. pressure and temperature (SiO_2, 1 wt%)

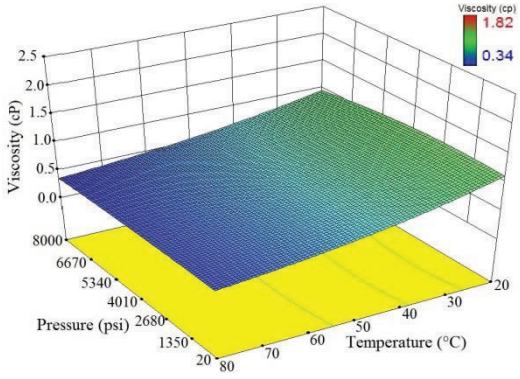

Figure 7d: 3D map of viscosity vs. pressure and temperature (SiO_2, 5 wt%)

INTERFACIAL TENSION (IFT) MEASUREMENTS

An Interfacial Tension Meter (IFT 700, manufactured by Vinci Technologies) was used to determine interfacial tension between the oil and DI water, polymer solution, and the nanofluid (liquid-liquid interface) at ambient (experimental) conditions. The pendant drop method was used for IFT measurements. An oil drop was created and put in contact with the nanofluid in a cell. A camera connected to a computer records the shape of the oil droplet to derive the interfacial tension. The results of IFT measurements are tabulated in Table 6 where the value reported is the average value for approximately 70 runs. The standard deviation was calculated for each test separately. As shown in the table, interfacial tension decreases significantly by adding nanoparticles to DI water. Moreover, the minimum IFT was obtained while using silica nanoparticles.

Table 6: Interfacial tension measurements

Fluid	**IFT (mN/m)**
DI Water and Oil	29.00
Silica nanofluid (5 wt%) and Oil	6.56 ± 1.06
Alumina nanofluid (5 wt%) and Oil	12.71 ± 0.35
Polymer Solution (10 ppm) and Oil	21.47 ± 1.30

CONCLUSIONS

In conclusion, the results of this experimental work shows that nanoparticle have the ability to increase oil recovery by improving both microscopic and macroscopic sweep efficiencies. The results of viscosity measurements demonstrated that alumina nanoparticles can increase the viscosity of deionized water. The viscosity of the silica and alumina nanofluids was measured at different conditions of pressure, temperature and nanoparticle concentration. Interfacial tension (IFT) experiments show that surface chemistry plays an important role when using nanoparticle enhanced water compared to polymer water solutions of the same viscosity in micromodel water flooding experiments. The results of IFT measurements indicate that the IFT between oil and DI water can decrease from 29 to 6.56 and 12.71 for silica (5 wt%) and alumina (5 wt%), respectively.

The results of micromodel experiments show that this IFT reduction causes higher oil recovery using nanofluid injection compared to polymer flooding with the polymer solution having the same viscosity as the nanofluids. Oil recoveries using polymer injection with concentrations of 10 and 20 ppm were 3 and 9% higher respectively than oil recovery using DI water injection, which shows the effect of viscosity improvement on oil recovery. The recoveries obtained from silica and alumina nanofluid injection were also higher than the recovery of DI water injection by 11 and 8% respectively. More investigation is required but our results indicate that surface chemistry does seem to play a role in oil recovery using nanofluids. This experimental work shows that nanoparticles are very promising for EOR purposes due to their specific chemical and physical properties, and the fact they have the ability to improve oil recovery through viscosity improvement and surface chemistry.

ACKNOWLEDGEMENTS

The authors thank the Hibernia Management and Development Company (HMDC), Chevron Canada, the Natural Sciences and Engineering Research Council of Canada (NSERC), and the Research and Development Corporation (RDC) for their support, without which this work could not have been performed.

REFERENCES

1. Chatzis, I., and Morrow, N. R., "Correlation of Capillary Number Relationships for Sandstone," *SPE Journal*, (1984) **24,** 05.
2. Lake, L. W., *Enhanced Oil Recovery*, Prentice Hall, New Jersey, USA, (1989).
3. Nguyen, P. T., Do, B. P. H., Pham, D. K., Nguyen, Q. T., Dao, D. Q .P., and Nguyen, H. A., "Evaluation on the EOR Potential Capacity of the Synthesized Composite Silica-Core/ Polymer-Shell Nanoparticles Blended with Surfactant Systems for the HPHT Offshore Reservoir Conditions," Paper presented at the SPE International Oilfield Nanotechnology Conference and Exhibition, 12-14 June, Noordwijk, The Netherlands, (2012).
4. Wang, J., Wang, D., Sui, X., Bai, W., "Combining Small Well Spacing with Polymer Flooding To Improve Oil Recovery of Marginal Reservoirs," SPE-96946-MS Paper presented at SPE/DOE Symposium on Improved Oil Recovery, 22-26 April, Tulsa, Oklahoma, USA, (2006).
5. Wang, Y., Zhao, F., Bai, B., "Optimized Surfactant IFT and Polymer Viscosity for Surfactant-Polymer Flooding in Heterogeneous Formations," SPE-127391-MS Paper presented at SPE Improved Oil Recovery Symposium, 24-28 April, Tulsa, Oklahoma, USA, (2010).
6. Morelato, P., Rodrigues, L., Romero, O. L., "Effect of Polymer Injection on the Mobility Ratio and Oil Recovery," SPE-148875-MS Paper presented at SPE Heavy Oil Conference and Exhibition, 12-14 December, Kuwait City, Kuwait, (2011).
7. Fletcher, A. J. P., Weston, S., Haynes, A. K., Clough, M. D., "The Successful Implementation of a Novel Polymer EOR Pilot in the Low Permeability Windalia Field," SPE-165253-MS Paper presented at SPE Enhanced Oil Recovery Conference, 2-4 July, Kuala Lumpur, Malaysia, (2013).

8. Kurenkov, V. F., Hartan, H. G., Lobanov, F. I., "Degradation of Polyacrylamide and Its Derivatives in Aqueous Solutions," *Russian Journal of Applied Chemistry*, (2002) **75**, 07, 1039-1050.
9. Ayatollahi, S. and Zerafat, M. M., "Nanotechnology-assisted EOR techniques: New solutions to old challenges," Paper SPE 157094 presented at the SPE International Oilfield Nanotechnology Conference and Exhibition, Noordwijk, 12-14 June, (2012).
10. Fei, D., Dingtian, K., and Alexandru, C., "Viscosity affected by nanoparticle aggregation in Al2O3-water nanofluids," *Nanoscale Research Letters*, (2011) **6**, 1, X1-5.
11. Zhi-Yong, L., Dong-Jian, S., Zhong-Qiang, Z., Jian-Ning, D., Guang-Gui, C., Long, Q., and Rui, Z., "Effect of temperature and nanoparticle concentration on the viscosity of nanofluids," *Gongneng Cailiao/Journal of Functional Materials*, (2013) **44**, 1, 92-95.
12. Maghzi, A., Mohebbi, A., Kharrat, R., and Ghazanfari, M. H., "Pore-scale monitoring of wettability alteration by silica nanoparticles during polymer flooding to heavy oil in a five-spot glass micromodel," *Transport in Porous Media*, (2011) **87**, 3, 653-664.
13. Roustaei, A., Moghadasi, J., Bagherzadeh, H., and Shahrabadi, A., "An Experimental Investigation of Polysilicon Nanoparticles Recovery Efficiencies through Changes in Interfacial Tension and Wettability Alteration," Paper SPE 156976 presented at the SPE International Oilfield Nanotechnology Conference and Exhibition, Noordwijk, 12-14 June, (2012).
14. Khezrnejad, A., James, L. A., and Johansen, T. E., "Water Enhancement Using Nanoparticles in Water Alternating Gas (WAG) Micromodel Experiments," Paper SPE 173484-STU presented at the SPE Annual Technical Conference and Exhibition, 27-29 October, Amsterdam, The Netherlands, (2014).
15. Zhang, T., Espinosa, D., Yoon, K. Y., Rahmani, A. R., Yu, H., Caldelas, F. M., Ryoo, S., Roberts, M., Prodanovic, M., Johnston, K. P., Milner, T. E., Bryant, S. L., and Huh, C., "Engineered Nanoparticles as Harsh-Condition Emulsion and Foam Stabilizers and as Novel Sensors," OTC-21212-MS Paper presented at Offshore Technology Conference, 2-5 May, Houston, Texas, USA, (2011).
16. Jafari, S., Khezrnejad, A., Shahrokhi, O., Ghazanfari, M. H., and Vossoughi, M., "Experimental Investigation of Heavy Oil Recovery by Continuous/WAG Injection of CO2 Saturated with Silica Nanoparticles. *International Journal of Oil, Gas and Coal Technology*, (2015) **9**, 2, 169-179.
17. Yu, J., Wang, S., Liu, N., and Lee, R., "Study of Particle Structure and Hydrophobicity Effects on the Flow Behavior of Nanoparticle-Stabilized CO2 Foam in Porous Media," Paper SPE-169047-MS presented at the SPE Improved Oil Recovery Symposium, 12-16 April, Tulsa, Oklahoma, USA, (2014).